# 11. IEEETEC2012_A Space-Vector Modulation Scheme for Multilevel

*by* Metta Savitri

**Submission date:** 13-Apr-2023 08:05AM (UTC-0500)
**Submission ID:** 2063428551
**File name:** IEEETEC2012_A_Space-Vector_Modulation_Scheme_for_Multilevel.pdf (1.24M)
**Word count:** 6070
**Character count:** 30872

# A Space-Vector Modulation Scheme for Multilevel Open-End Winding Five-Phase Drives

Emil Levi, *Fellow, IEEE*, I Nyoman Wahyu Satiawan, Nandor Bodo, *Student Member, IEEE*, and Martin Jones

*(Invited Paper)*

***Abstract*—Open-end winding three-phase variable speed drives with dual-inverter supply have been extensively investigated for various applications, including series hybrid powertrains and propulsion motors. The topology is simple to realize while offering a higher number of switching states without the need for capacitor voltage balancing algorithms, when compared to the standard multilevel converters. This paper extends the open-end winding concept to a five-phase drive. A relatively simple space-vector modulation (SVM) algorithm, based on the already well-understood five-phase two-level drive SVM method, is developed. The proposed modulation technique has the advantage of being straightforward to implement and, like its two-level counterpart, is able to generate output voltages with minimum low-order harmonic content. The method generates up to 17-level output phase voltage and, therefore, offers superior harmonic performance when compared to the two-level five-phase modulation. The developed scheme is verified via detailed simulations and experiments, using a five-phase induction machine operating under open-loop *V/f* control.**

***Index Terms*—Induction motor drives, multiphase ac drives, open-end winding, space vector modulation.**

## I. Introduction

THE concept of cascading two voltage source inverters (VSIs), one at each side of an open-end stator winding, is well known [1]. Typically, two two-level three-phase VSIs are utilized. Application of such a dual-inverter supply enables drive operation with voltage waveform equivalent to the one obtainable with a three-level VSI in single-sided supply mode. Three-phase open-end winding dual-inverter fed drive systems are currently considered as possible alternative supply solutions in electric vehicles and hybrid electric vehicles (EVs/HEVs) [2]–[5], for electric ship propulsion [6], rolling mills [7], etc. Recently research efforts have been directed toward the use of this supply configuration in renewable electric energy systems [8].

In applications such as EVs, where dc-link voltage is rather low and limited, the main reported advantage with respect to the equivalent multilevel single-sided supply is that a machine with a lower current rating can be utilized since the voltage across phases can be higher when two independent batteries are used instead of a single one [2], [5]. Assuming that both inverters are two-level, the number of the switches is the same as in the equivalent three-level single-sided supply. However, additional diodes used in the neutral-point-clamped (NPC) VSI are not needed, leading to a saving in the overall number of components. Also, the problem of capacitor voltage balancing does not exist if the supply is two-level at each winding side. Thus, the implementation cost is slightly lower, when compared to the equivalent three-level inverter application, and the implementation is simpler. A further important advantage of the open-end winding topology is much improved fault tolerance, since in case of a failure in one inverter it can be shut down and the operation continued with only the other, healthy inverter in single-sided supply mode.

Multiphase ($n$-phase) variable-speed drive systems are currently regarded as another category of potentially viable solutions for the same applications, including EVs/HEVs [9]. A two-level multiphase VSI is the standard solution, and the machine winding is star-connected, with an isolated neutral point. The advantages of multilevel inverters and multiphase drives complement each other so that it appears to be beneficial to try to combine them by realizing a multilevel multiphase drive system. There are, however, currently very few examples [10]–[21] of such topologies.

Recently, some research effort has been directed toward the multiphase open-end winding topology [10]–[14]. An asymmetrical six-phase induction motor drive has been developed in [10] and [11]. In [10], the supply is provided by means of two isolated two-level six-phase VSIs. The goal was in essence low-order harmonic elimination/reduction rather than the multilevel operation so that the dual converter is not operated in multilevel mode. The topology elaborated in [11] uses four three-phase two-level inverters, with four isolated dc sources, to prevent circulation of zero sequence currents. The space-vector modulation (SVM) control is performed in essence independently for the two three-phase windings, using the nearest three-vector approach in conjunction with the three-level inverter. This study is focused on controlling the power sharing between the four converters. The five-phase configuration has been examined in [12] and [13] and a suitable SVM algorithm has been proposed. In [14], the SVM algorithm developed in [13] is extended to the seven-phase configuration.

The remaining literature primarily deals with the five-phase three-level VSI supplied drive in single-sided supply mode

Manuscript received August 25, 2011; accepted November 11, 2011. Date of publication December 30, 2011; date of current version February 17, 2012. This work was supported by the Qatar National Research Fund (QNRF) under Project NPRP 4-152-2–053. Paper no. TEC-00450-2011.

The authors are with the School of Engineering, Technology and Maritime Operations, Liverpool John Moores University, Liverpool, L3 3AF, U.K. (E.Levi@ljmu.ac.uk; I.N.Satiawan@2008.ljmu.ac.uk; N.Bodo@2009.ljmu.ac.uk; M.Jones2@ljmu.ac.uk).

Color versions of one or more of the figures in this paper are available online at http://ieeexplore.ieee.org.

Digital Object Identifier 10.1109/TEC.2011.2178074

[15]–[21]. The first SVM techniques for multilevel multiphase VSIs were based on the simple extension of the three-phase SVM approaches so that only the three vectors, nearest to the reference, were utilized. Such an extension from the three-phase to five-phase system, which divides each sector into four equal triangles, is given for a three-level inverter in [16]. An optimal SVM switching strategy, based on modified discrete particle swarm optimization (PSO), is presented in [15]. In principle, the number of applied vectors must equal the number of phases [9]. Utilization of three instead of five space vectors during the switching period disregards this basic rule; consequently, only the first plane of the multiphase system is controlled. Hence, numerous low-order harmonics are generated, which map into the second plane. An SVM method, which controls both planes, has been developed in [17] for the three-level NPC VSI supplied five-phase drive and it was extended to the seven-phase case in [18]. The SVM method is complicated, particularly the subsector identification, since each 36° sector is partitioned into ten subsectors in [17]. A different approach to the SVM of multilevel multiphase systems is given for a general case of an $m$-level, $n$-phase VSI in [19] and [20]. The algorithm is based on the considerations of the multidimensional ($n$-dimensional) space and, therefore, does not include decomposition of the $n$-dimensional space into 2-D planes. A somewhat similar method, in the sense that decomposition into 2-D planes is not utilized, is the one in [21], where a multiphase multilevel pulse width modulation (PWM) is developed using $n$ single-leg modulators.

Theoretical principles of the SVM algorithm, considered here, have been originally developed by the authors in [13] for the five-phase open-end winding configuration. This paper enhances the work of [13] by providing an in-depth analysis of the SVM subsectors, results of a detailed simulation study of the drive system, and experimental results collected from the laboratory prototype of an open-end five-phase induction motor drive. The method is relatively straightforward to understand and implement since it is based on the previously developed SVM method for two-level five-phase converters. General properties of the five-phase ac motor drives with sinusoidal winding distribution are at first reviewed, along with an available two-level SVM algorithm for a five-phase two-level VSI [22], which uses two large and two medium active space vectors per switching period in order to minimize low-order harmonics. Next, mathematical model of the open-end winding topology is given, along with mapping of the space vectors that are of interest into the torque-producing 2-D subspace. The performance of the open-end winding five-phase drive is investigated and verified using detailed simulation and experimental results.

## II. Preliminary Considerations

Prior to considering the SVM schemes for the open-end winding topology, it is beneficial to review the basic relationships, which govern the performance of five-phase drives and the corresponding two-level SVM technique for a five-phase VSI. A five-phase machine with near-sinusoidal magnetomotive force distribution can be modeled in two 2-D subspaces, termed $\alpha$–$\beta$ and $x$–$y$ subspaces [9]. It can be shown that only current harmonic components, which map into the $\alpha$–$\beta$ subspace develop useful torque and torque ripple, whereas those that map into the $x$–$y$ subspace do not contribute to the torque at all. Such a multiphase machine presents extremely low impedance to all nonflux/torque producing supply harmonics and it is, therefore, mandatory that the supply does not generate these harmonics. What this means is that the design of a five-phase PWM strategy must consider simultaneously both 2-D subspaces, where the reference voltage, assuming pure sinusoidal references, is in the first plane while reference in the other plane is zero. Two-level five-phase inverters can generate up to $2^5 = 32$ voltage space vectors with corresponding components in the $\alpha$–$\beta$ and $x$–$y$ subspaces, as shown in Fig. 1. Space vectors are labeled with decimal numbers, which, when converted into binary, reveal the values of the switching functions of each of the inverter legs. Active

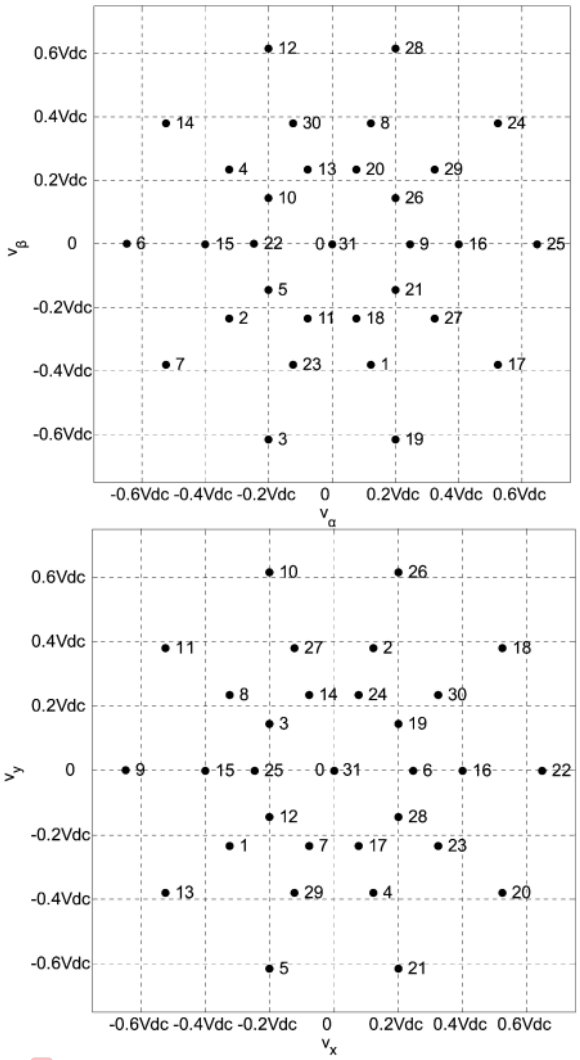


Fig. 1. Two-level five-phase VSI space vectors in the $\alpha$–$\beta$ and $x$–$y$ planes.

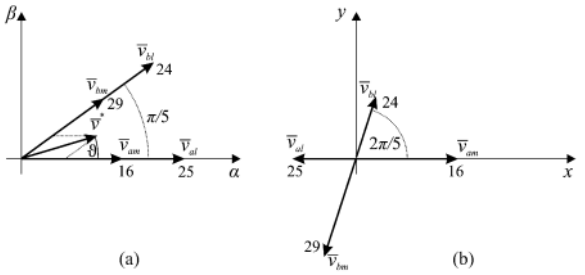


Fig. 2. Principle of calculation of times of application of the active space vectors (vectors are shown in the $\alpha$–$\beta$ (a) and $x$–$y$ (b) planes and the reference in the $x$–$y$ plane equals zero).

(nonzero) space vectors belong to three groups in accordance with their magnitudes—small, medium, and large space vector groups. The magnitudes are identified with indices $s$, $m$, and $l$ and are given as $|\bar{v}_s| = 4/5\cos(2\pi/5)V_{\rm dc}$, $|\bar{v}_m| = 2/5V_{\rm dc}$, and $|\bar{v}_l| = 4/5\cos(\pi/5)V_{\rm dc}$, respectively. Four active space vectors are required to generate sinusoidal voltages [9]. Suppose that the reference space vector in the $\alpha$–$\beta$ plane is in sector $s = 1$ [see Fig. 2(a)]. Two neighboring large and two medium space vectors are selected. In order to provide zero average voltage in the $x$–$y$ plane [see Fig. 2(b)] times of application of active space vectors become [22]

$$t_{al} = \frac{2\sin(2\pi/5)}{V_{\rm dc}} \sin\left(s\frac{\pi}{5} - \theta\right)|\bar{v}^*|t_s$$
$$t_{am} = \frac{2\sin(\pi/5)}{V_{\rm dc}} \sin\left(s\frac{\pi}{5} - \theta\right)|\bar{v}^*|t_s \quad (1)$$

$$t_{bl} = \frac{2\sin(2\pi/5)}{V_{\rm dc}} \sin\left[\theta - (s-1)\frac{\pi}{5}\right]|\bar{v}^*|t_s$$
$$t_{bm} = \frac{2\sin(\pi/5)}{V_{\rm dc}} \sin\left[\theta - (s-1)\frac{\pi}{5}\right]|\bar{v}^*|t_s \quad (2)$$

where $t_s$ is the switching period, $\theta$ is the reference position, $s$ is the sector number, and indices $a$ and $b$ are defined in Fig. 2(a). Total time of application of the zero space vector $t_0 = t_s - (t_{al} + t_{am} + t_{bl} + t_{bm})$ is equally shared between two zero states $\bar{v}_0$ and $\bar{v}_{31}$. The maximum peak value of the output fundamental phase-to-neutral voltage in the linear modulation region is $v_{\rm max} = V_{\rm dc}/[2\cos(\pi/10)] = 0.525V_{\rm dc}$ (i.e., $M_{\rm max} = 1.05$) [22]. Switching pattern is a symmetrical PWM with two commutations per each inverter leg.

## III. Five-Phase Open-End Winding Topology

Fig. 3 illustrates the open-end winding structure, based on utilization of two two-level five-phase VSIs. The two inverters are identified with indices 1 and 2. Inverter legs are denoted with capital letters *A*,*B*,*C*,*D*,*E* and the negative rails of the two dc links are identified as *N*1 and *N*2. Machine phases are labeled as *a*,*b*,*c*,*d*,*e*. Phase voltage positive direction is with reference to the left inverter (inverter 1). Using the notation of Fig. 3, phase

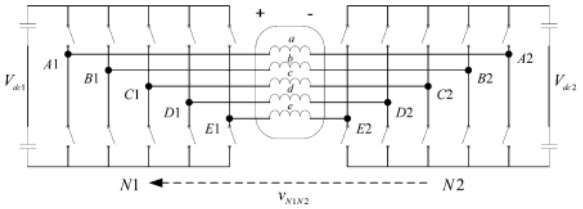


Fig. 3. Five-phase machine with dual two-level inverter supply.

voltages of the stator winding can be given as follows:

$$v_a = v_{A1N1} + v_{N1N2} - v_{A2N2}$$
$$v_b = v_{B1N1} + v_{N1N2} - v_{B2N2}$$
$$v_c = v_{C1N1} + v_{N1N2} - v_{C2N2}$$
$$v_d = v_{D1N1} + v_{N1N2} - v_{D2N2}$$
$$v_e = v_{E1N1} + v_{N1N2} - v_{E2N2}. \quad (3)$$

Two isolated dc supplies are assumed so that the common mode voltage (CMV) $v_{N1N2}$ is of nonzero value (the issue of CMV elimination is not addressed here). The resulting space vectors in dual-inverter supply mode will depend on the ratio of the two dc-link voltages. The situation considered further on is the setting $V_{\rm dc1} = V_{\rm dc2} = V_{\rm dc}/2$. This gives the equivalent of the single-sided three-level supply with dc-link voltage equal to $V_{\rm dc}$. Since in the five-phase case single-sided supply gives nine levels in the phase voltages, it is expected that with dual-inverter supply there will be up to 17 levels in the phase voltage. The increased number of phase voltage levels is a consequence of the much greater number of switching states and voltage space vectors (1024 and 211, respectively), generated by the converter, when compared to the single-sided supply mode.

Space vectors of phase voltages in the two planes are determined with

$$\bar{v}_{\alpha-\beta} = \left(\frac{2}{5}\right)\left(v_a + \bar{a}v_b + \bar{a}^2v_c + \bar{a}^3v_d + \bar{a}^4v_e\right)$$
$$\bar{v}_{x-y} = \left(\frac{2}{5}\right)\left(v_a + \bar{a}^2v_b + \bar{a}^4v_c + \bar{a}^6v_d + \bar{a}^8v_e\right) \quad (4)$$

where $\bar{a} = \exp(j2\pi/5)$. Using (3) and (4), one gets

$$\bar{v}_{\alpha-\beta} = \bar{v}_{\alpha-\beta(A1B1C1D1E1)} - \bar{v}_{\alpha-\beta(A2B2C2D2E2)}$$
$$\bar{v}_{x-y} = \bar{v}_{x-y(A1B1C1D1E1)} - \bar{v}_{x-y(A2B2C2D2E2)}. \quad (5)$$

When developing a suitable SVM strategy for the dual-inverter supply and considering (5), it seems logical to adapt the two-level SVM method for the five-phase VSI of [22] accordingly. Considering that the two-level SVM method uses only large and medium active vectors during each switching period and these can now be applied from each side, there are nine possible vector combinations, as illustrated in Fig. 4. The nine vector combinations result in a total of 131 phase voltage space vector positions. Since there are $22 \times 22 = 484$ possible switching states, disregarding the small vectors, there are 353 redundant switching states. The space vector lengths and positions, in the

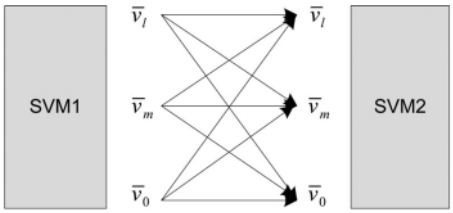


Fig. 4. Five-phase dual-inverter switching combinations.

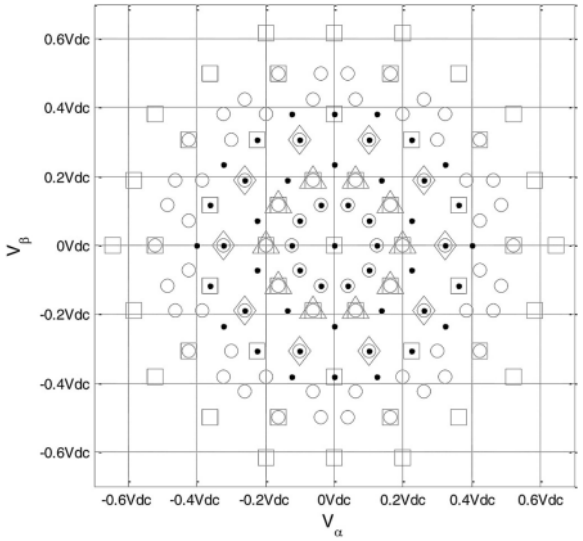


Fig. 5. Space vectors in $\alpha$–$\beta$ plane, created by $\bar{v}_l - \bar{v}_l$ (□), $\bar{v}_m - \bar{v}_m$ (•), $\bar{v}_m - \bar{v}_l$, $\bar{v}_l - \bar{v}_m$ (○), $\bar{v}_l - \bar{v}_0$, $\bar{v}_0 - \bar{v}_l$ (◇), $\bar{v}_m - \bar{v}_0$, $\bar{v}_0 - \bar{v}_m$ (Δ) combinations.

$\alpha$–$\beta$ subspace, generated by these vector combinations, are presented in Fig. 5 (zero–zero combination is omitted). The high level of redundancy, which exists, offers great scope for optimizing the performance of the converter, including power sharing. The development of such algorithms is, however, beyond the scope of this paper and is postponed for further work.

## IV. Space Vector Modulation Method

The basic idea of [13] is to decompose the problem of space vector PWM of the complete system into two subproblems of lower level complexity, by splitting the total reference into individual references of the two inverters. By doing so, it becomes possible to apply well-known SVM methods for two-level inverters [22] to two individual two-level inverters at each end of the winding. The SVM scheme, suggested in [13] and illustrated in Fig. 6, uses two identical two-level modulators. It is interesting to note that two-level multiphase SVM methods employ the same space vectors for the same dwell times as one carrier-based PWM method [23] and, thus, give the same results in terms of phase and line-to-line voltages. This equivalent carrier-based PWM method is the one with offset injection (i.e., zero-sequence signal injection), defined as $v_{zs} = -0.5(\max\{v_j^*\} + \min\{v_j^*\})$,

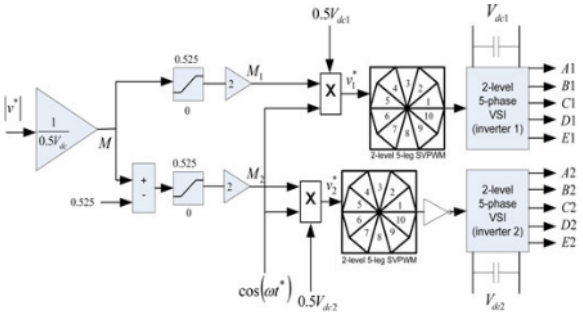


Fig. 6. Unequal reference sharing scheme.

$j = a,b,c,d,e$. Therefore, it can be concluded that the individual two-level modulators of Fig. 6 may also use the carrier-based approach, with inverted carriers for the inverter 2 modulator. It, thus, follows that the simulation and experimental results presented in this paper for the SVM are equally applicable to the carrier-based two-level modulation method with offset injection.

The voltage reference applied to the two-level modulators is apportioned according to the modulation index $M$. For clarity, it is beneficial to define individual modulation indices as $M_1 = v_1^*/(0.5V_{\mathrm{dc1}}), M_2 = v_2^*/(0.5V_{\mathrm{dc2}})$. Only inverter 1 is operational up to the point when $M = 0.525$ ($M_1 = 1.05$). Hence, the converter operates in two-level mode, since inverter 2 is not modulated and the VSI is locked in a zero switching state 11111 or 00000, forming a neutral point. It is shown further on that the performance is significantly improved compared to the two-level single-sided configuration. When $M > 0.525$, inverter 1 is held at $M_1 = 1.05$ and inverter 2 output is modulated as well. These constraints can be expressed as follows:

$$\begin{aligned} 0 \le M \le 0.525 \quad & \begin{cases} M_1 = 2M \\ M_2 = 0 \end{cases} \\ 0.525 < M \le 1.05 \quad & \begin{cases} M_1 = 1.05 \\ M_2 = 2(M - 0.525). \end{cases} \end{aligned} \tag{6}$$

Unequally apportioning the voltage reference between the two modulators leads to multilevel operation and improved harmonic performance when compared to the equivalent two-level method in single-sided supply mode [13].

It should be noted that both inverters operate with the same switching frequency in the range $M > 0.525$ and hence the switching losses are equally distributed. In the region of $M$ up to 0.525, where only one inverter is used, it is possible to concentrate the switching losses to the same inverter, by keeping the other one at all times in the zero state, or to equalize the switching losses by alternating the inverter used to produce the output voltage.

## V. Switching Trajectories

The space-vectors applied by each inverter are predetermined for any given sector. However, the applied space vectors seen from the perspective of the machine will alter depending on the modulation indices and the angular position within the

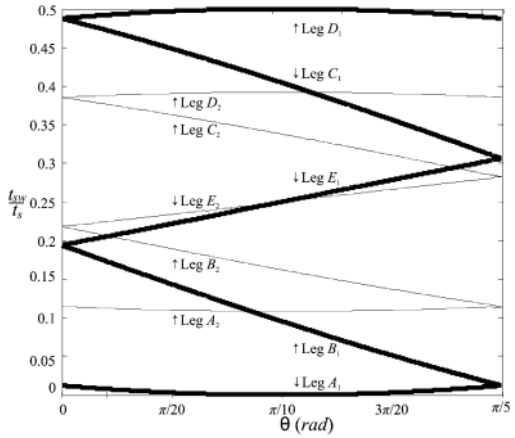


Fig. 7. Normalized inverter leg switching instants for sector 1, $M = 0.82$.

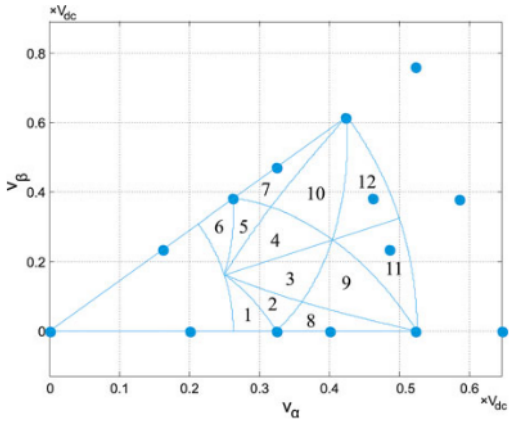


Fig. 8. Subsectors of sector 1 and the applied space vectors.

sector, since the modulation indices are not the same for the two inverters (except when $M = M_{\max} = 1.05$). Fig. 7 shows the normalized switching instants (turn-ON and turn-OFF instants for inverters 1 and 2, respectively), in the first half of the switching period, of each inverter leg for every angular position in the first sector, when $M = 0.82$ so that $M_1 = M_{\max} = 1.05$ (thick lines) and $M_2 = 0.59$ (thin lines). These switching instants are determined by the reference signals for each leg. The border where the change of the switching sequence appears is governed by the intersection of the thick and thin lines in Fig. 7. By considering a carrier-based approach and taking into account the equations of the carriers, the intersection of the switching instants can be calculated using

$$t_{\mathrm{sw}-1} = \frac{1 - v_{l1}^*}{4} \qquad t_{\mathrm{sw}-2} = \frac{1 + v_{l2}^*}{4} \tag{7}$$

where $v_{li}^*$ is the reference signal for leg $l$ ($l = 1,2\ldots5$) of the inverter $i$ ($i = 1,2$). The reference signals used in the modulation are sinusoidal signals with added offset injection, which can be given in per unit as follows:

$$v_{l1}^* = M_{\max}[\cos(\theta - (l_1 - 1)\alpha) + v_{zs}^{\mathrm{pu}}] \tag{8}$$

$$v_{l2}^* = -M_2[\cos(\theta - (l_2 - 1)\alpha) + v_{zs}^{\mathrm{pu}}] \tag{9}$$

where $\alpha = 2\pi/5$, and $l_1$ and $l_2$ take the values 1,2…5. Offset injection $v_{zs}^{\mathrm{pu}}$ is determined in the first sector at modulation index equal to one, where references of phases $a$ and $d$ are at maximum and minimum, respectively, as

$$v_{zs}^{\mathrm{pu}} = -0.5\,(\cos(\theta - (1-1)\alpha) + \cos(\theta - (4-1)\alpha). \tag{10}$$

The switching instants are, therefore, determined as follows:

$$t_{\mathrm{sw}-1} = \frac{1 - M_{\max}[\cos(\theta - (l_1 - 1)\alpha) + v_{zs}^{\mathrm{pu}}]}{4} \tag{11}$$

$$t_{\mathrm{sw}-2} = \frac{1 - M_2[\cos(\theta - (l_2 - 1)\alpha) + v_{zs}^{\mathrm{pu}}]}{4}. \tag{12}$$

The switching instants have variable values, depending on the modulation index and angular position of the reference. There is

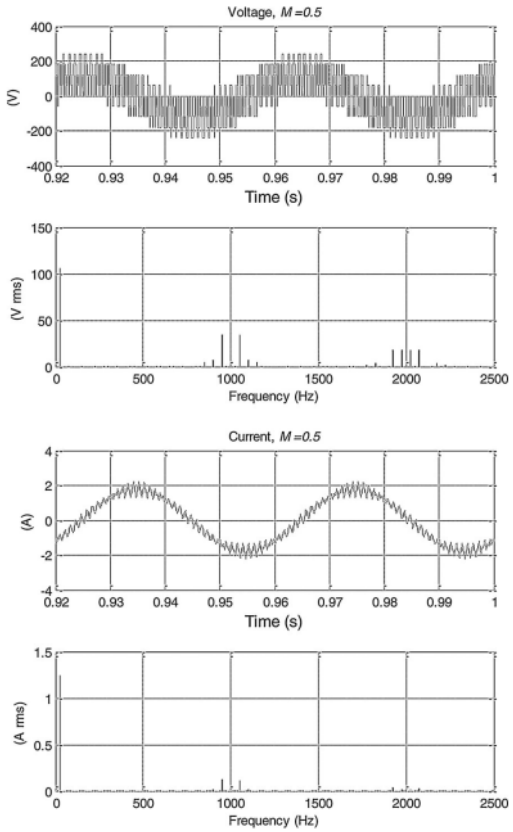


Fig. 9. Motor phase voltage and current waveforms with spectra, $M = 0.5$.

a change in the resultant applied space vectors as switching instants change their order. These situations lead to a transfer from one subsector to another. Obviously, the borders of the subsectors are determined by having two switching instants equal. A computer program is developed to calculate $M_2$ for each angular

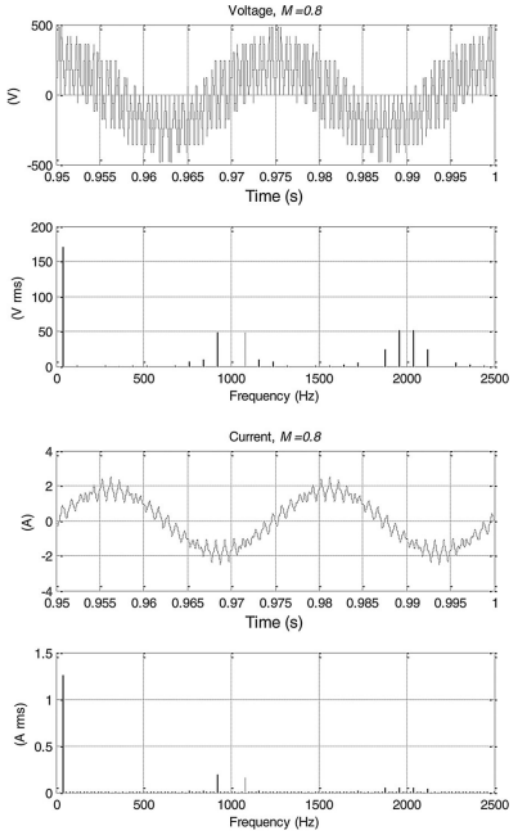


Fig. 10. Motor phase voltage and current waveforms with spectra, $M = 0.8$.

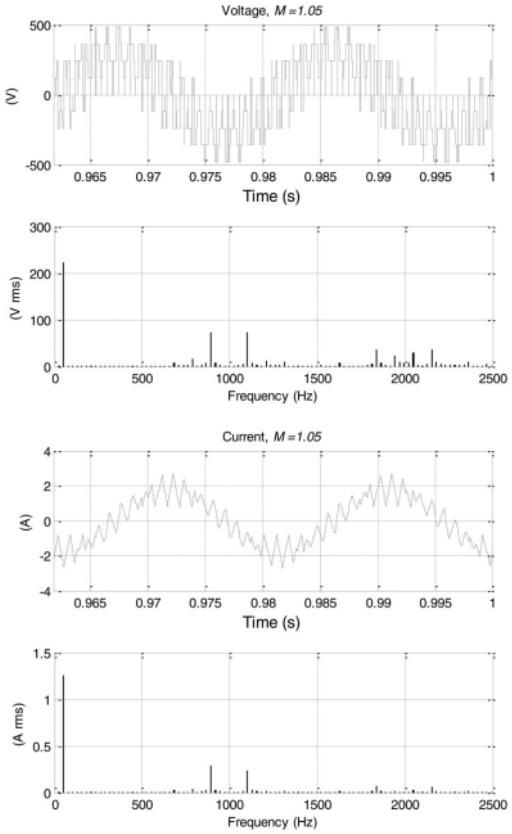


Fig. 11. Motor phase voltage and current waveforms with spectra, $M = 1.05$.

position $\theta$, according to

$$M_2 = M_{\max} \frac{(\cos(\theta - (l_1 - 1)\alpha) + v_{zs}^{\mathrm{pu}})}{(\cos(\theta - (l_2 - 1)\alpha) + v_{zs}^{\mathrm{pu}})}. \quad (13)$$

The corresponding values of $M_2$ are calculated for each $\theta$ and the resulting values can be plotted as a complex number $\bar{Z}$, given as follows:

$$\bar{Z} = Me^{j\theta} \qquad M = \frac{(M_{\max} + M_2)}{2}. \quad (14)$$

The resulting subsectors can be seen in Fig. 8 for sector 1. There are 12 subsectors in multilevel mode, meaning that there are 12 different switching sequences depending on the modulation index $M$ and the angular position of the reference. The identification of the subsectors together with the large number of switching sequences make the creation of a single equivalent SVM modulator somewhat difficult to achieve.

## VI. Simulation Verification

In order to verify the drive's performance, a series of simulations were undertaken. The phase variable model of the five-phase induction machine [24] is used and the drive is operated in open-loop *V/f* mode. The switching frequency of each inverter is set to 1 kHz and each dc link is 300 V, giving an effective dc-link voltage of 600 V when $M > 0.525$. Dead time and other nonideal effects of the inverter are not modeled.

The stator phase voltage and current waveforms and their spectra are presented in Fig. 9 when $M = 0.5$. As indicated in (6), the drive operates with only one inverter being modulated while the other is clamped to the zero switching vector, hence the drive operates in two-level mode and the phase voltage has nine levels. The 50% reduction in the effective dc-link voltage is evident in the phase voltage waveform. This reduction of the effective dc-link voltage leads to a much improved voltage and current total harmonic distortion (THD) when compared to the equivalant single inverter supplied two-level drive [13]. The situation when $M = 0.8$ is shown in Fig. 10. Both inverters are now modulated according to (6) and the effective dc-link voltage is now 600 V. The phase voltage now comprises 17 levels. The phase voltage levels are equidistanly spaced, i.e., the step is 60 V. However, it is fair to say that the drive achieves a pseudomultilevel output since the phase voltage switches to zero throughout the fundamental cycle, in contrast to a true multilevel waveform. Fig. 11 illustrates the case when $M = 1.05$ and both inverters are operating at the maximum modulation index. The inverters are now synchronized and the drive operates in two-level mode with nine levels in the phase voltages. It can be seen that effective dc-link voltage is again 600 V and the voltage

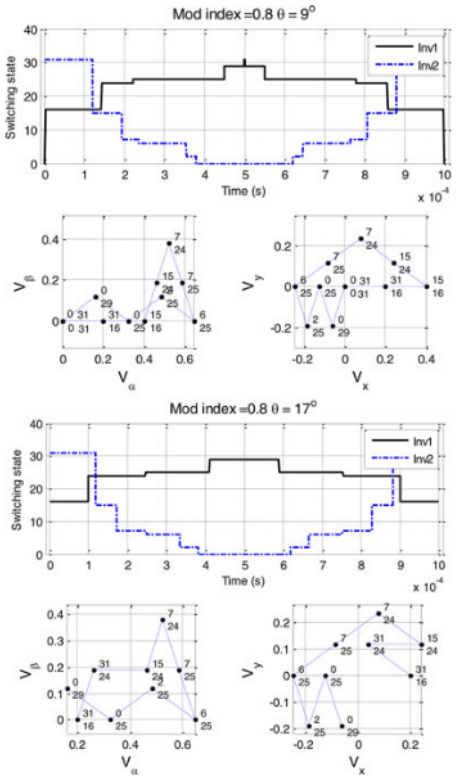


Fig. 12. Inverter switching trajectories in the $\alpha$–$\beta$ and $x$–$y$ planes for $M = 0.8$ with reference angular positions of 9° and 17° in the $\alpha$–$\beta$ plane.

steps are now 120 V. In all cases the spectra indicate that the low-order harmonic content is the lowest possible and the target fundamental voltages have been met.

Finally, the switching trajectories of the drive along with the switching state of each inverter, for the case when $M = 0.8$ and the reference angular position is $\theta = 9°$ and $\theta = 17°$ in sector 1 of the $\alpha$–$\beta$ plane, are shown in Fig. 12. These positions correspond to the reference being in subsectors 9 and 3 of Fig. 8, respectively. The vectors are numbered in the same manner as in Fig. 1, the upper number being inverter 2 and the lower number inverter 1. It can be seen that nine active vectors are applied during each switching period. As expected, the switching trajectory changes with inverter 2 no longer applying a zero vector when $\alpha = 17°$ and the vector 15–16 is no longer applied and is replaced with vector 31–24 from inverters 2 and 1, respectively. Further simulations show that five active vectors are applied when the reference coincides with the sector borders (when $\theta = k{\cdot}36°$, $k = 0,1,2\ldots9$).

## VII. Experimental Verification

The experimental results are obtained using two custom built five-phase two-level VSIs and a four-pole five-phase induction motor. Each stator phase consists of two half-windings, which can be connected in series or in parallel [25]. In this study the half-windings are series-connected. Parameters of this motor

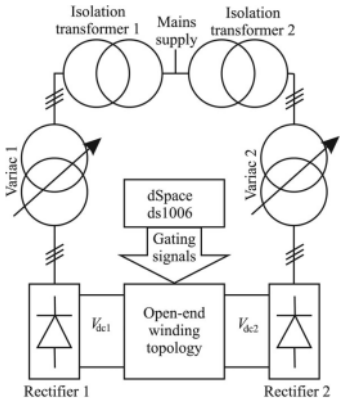


Fig. 13. Outlay of the experimental setup.

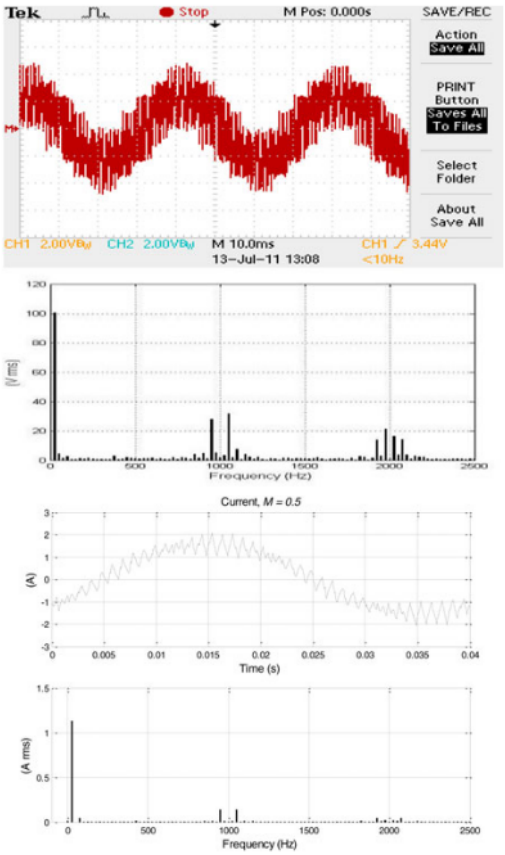


Fig. 14. Experimental results: stator phase voltage and current with spectra when $M = 0.5$.

have been used in the simulation study of Section VI. The inverters are controlled using a dSpace DS1006 processor board. The dSpace module is connected to the VSIs via a dSpace DS5101 digital waveform unit. Both VSIs are fed with isolated three-phase 212 V rms line-to-line voltage, through diode bridge rectifiers. The outlay of the experimental setup is shown

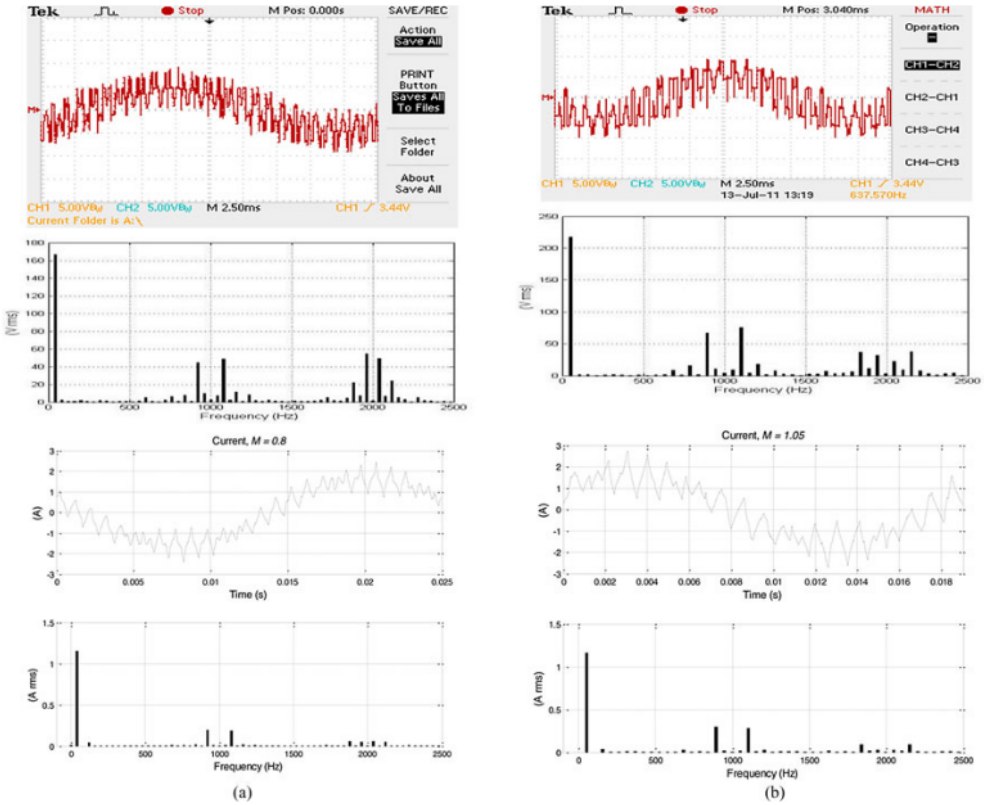


Fig. 15. Experimental results: stator phase voltage and current with spectra when $M = 0.8$ (a) and $M = 1.05$ (b).

in Fig. 13, while a photograph is given in Fig. A1. The motor is controlled in open-loop *V*/*f* mode with the maximum modulation index ($M = 1.05$) being reached when the fundamental frequency is 52.5 Hz. The switching frequency of each inverter is 1 kHz and the dead time is approximately 6 $\mu$s. The phase voltages are measured using a Tektronix digital oscilloscope in differential mode and a voltage divider, which gives an attenuation of 52. The current measurements are recorded using a Tektronix current probe and a HP35665A dynamic signal analyzer. The spectra are calculated using MATLAB software.

Fig. 14 depicts the experimental results obtained when $M = 0.5$ and the drive operates in two-level mode. It can be seen that the effective dc-link voltage is approximately 300 V. The phase voltage comprises nine levels and the target fundamental has been met. Performance of the drive when $M = 0.8$ and $M = 1.05$ is presented in Fig. 15. The drive now utilizes both inverters, so the effective dc-link voltage is approximately 600 V. When $M = 0.8$, the drive operates in multilevel mode. Upon inspection, 15 voltage levels can be identified. This is less than indicated by the simulation results; however, dead time and other nonlinear effects are ignored in the simulations and can account for the missing levels. Overall the experimental results agree very well with the simulation results. Some small low-order harmonics (in particular, the third) can be seen in the voltage and current spectra, which are again a consequence of the nonideal nature of the experimental setup (dead-time effect, as discussed in [25]).

## VIII. Conclusion

This paper has presented an SVM method for the dual-inverter five-phase open-end winding topology, which is relatively easy to implement. The scheme utilizes two standard five-phase two-level SVM modulators, one for each inverter, and apportions the voltage reference unequally between the two inverters. As long as the total modulation index is $M \leq 0.525$, only one inverter output is modulated while the other inverter is held in zero state. Once when $M > 0.525$ both inverter outputs are modulated, with inverter 1 held at its maximum modulation index ($M_1 = 1.05$). The performance of the five-phase open-end winding drive has been verified by simulation and experimentally. The results confirm that the load phase voltage waveform has an increasing number of levels, from only nine when just inverter 1 is operational (with inverter 2 held in zero state) up to, theoretically, 17 levels when both inverters are operational.

Finally, it should be noted that, although *V*/*f* control was studied here, the principle of SVM is directly applicable to all vector control schemes, which operate with current control in the rotating reference frame so that the control system output

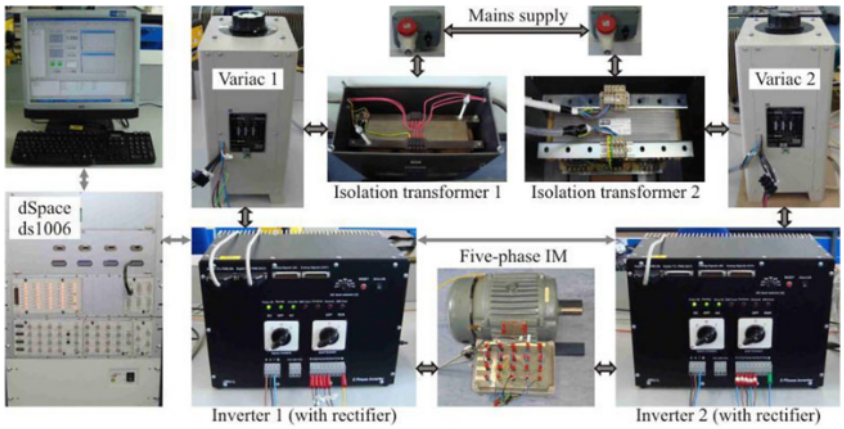


Fig. A1. Experimental setup.

is the stator voltage reference. It is only necessary to apportion the total stator voltage reference using (6) in order to realize the vector controlled operation.

## APPENDIX

The experimental setup is shown in Fig. A1, at the top of the page.

## REFERENCES

[1] H. Stemmler and P. Guggenbach, "Configurations of high-power voltage source inverter drives," in *Proc. Eur. Power Elec. Appl. Conf.*, Brighton, U.K., 1993, vol. 5, pp. 7–14.

[2] C. Rossi, G. Grandi, P. Corbelli, and D. Casadei, "Generation system for series hybrid powertrain based on dual two-level inverter," in *Proc. Eur. Power Elec. Conf.*, Barcelona, Spain, 2009 [CD-ROM], Paper 0978, pp. 1–10.

[3] D. Casadei, G. Grandi, A. Lega, and C. Rossi, "Multi-level operation and input power balancing for a dual two-level inverter with insulated dc sources," *IEEE Trans. Ind. Appl.*, vol. 44, no. 6, pp. 1815–1824, Nov./Dec. 2008.

[4] B. A. Welchko and J. M. Nagashima, "A comparative evaluation of motor drive topologies for low-voltage, high-power EV/HEV propulsion systems," in *Proc. IEEE Int. Symp. Ind. Elec.*, Rio de Janerio, Brazil, 2003, pp. 379–384.

[5] G. Griva, V. Oleschuk, and F. Profumo, "Hybrid traction drive with symmetrical split phase motor controlled by synchronised PWM," in *Proc. Int. Symp. Power Electron., Electr. Drives, Autom. Motion*, Ischia, Italy, 2008, pp. 1033–1037.

[6] G. Grandi, C. Rossi, A. Lega, and D. Casadei, "Multi-level operation of a dual two-level inverter with power balancing capability," in *Proc. IEEE Ind. Appl. Soc. Ann. Meet.*, Tampa, FL, 2006, pp. 603–610.

[7] Y. Kawabata, M. Nasu, T. Nomoto, E. C. Ejiogu, and T. Kawabata, "High-efficiency and low acoustic noise drive system using open-winding AC motor and two space-vector-modulated inverters," *IEEE Trans. Ind. Electron.*, vol. 49, no. 4, pp. 783–789, Aug. 2002.

[8] G. Grandi, C. Rossi, D. Ostojic, and D. Casadei, "A new multi-level conversion structure for grid-connected PV applications," *IEEE Trans. Ind. Electron.*, vol. 56, no. 11, pp. 4416–4426, Nov. 2009.

[9] E. Levi, "Multi-phase electric machines for variable-speed applications," *IEEE Trans. Ind. Electron.*, vol. 55, no. 5, pp. 1893–1909, May 2008.

[10] K. K. Mohapatra and K. Gopakumar, "A novel split phase induction motor drive without harmonic filters and with linear voltage control for the full modulation range," *EPE J.*, vol. 16, no. 4, pp. 20–28, 2006.

[11] G. Grandi, A. Tani, P. Sanjeevikumar, and D. Ostojic, "Multi-phase multi-level AC motor drive based on four three-phase two-level inverters," in *Proc. Int. Symp. Power Electron., Electr. Drives, Autom. Motion*, Pisa, Italy, 2010, pp. 1768–1775.

[12] E. Levi, M. Jones, and W. Satiawan, "A multi-phase dual-inverter supplied drive structure for electric and hybrid electric vehicles," in *Proc. IEEE Vehicle Power Propulsion Conf.*, Lille, France, 2010 [CD-ROM], Paper 95-45630, pp. 1–7.

[13] M. Jones, W. Satiawan, and E. Levi, "A five-phase multilevel space-vector PWM algorithm for a dual-inverter supplied drive," in *Proc. IEEE Ind. Elec. Soc. Annu. Meet.*, Glendale, AZ, 2010, pp. 2461–2466.

[14] N. Bodo, M. Jones, and E. Levi, "Multi-level space-vector PWM algorithm for seven-phase open-end winding drives," in *Proc. IEEE Int. Symp. Ind. Elec.*, Gdansk, Poland, 2011, pp. 1881–1886.

[15] C. M. Hutson, G. K. Venayagamoorthy, and K. A. Corzine, "Optimal SVM switching for a multilevel multi-phase machine using modified discrete PSO," in *Proc. IEEE Swarm Intell. Symp.*, St. Louis, MO, 2008 [CD-ROM], pp. 1–6.

[16] Q. Song, X. Zhang, F. Yu, and C. Zhang, "Research on PWM techniques of five-phase three-level inverter," in *Proc. Int. Symp. Power Elec., Electr. Drives, Autom. Motion*, Taormina, Italy, 2006, pp. 561–565.

[17] L. Gao and J. E. Fletcher, "A space vector switching strategy for three-level five-phase inverter drives," *IEEE Trans. Ind. Electron.*, vol. 57, no. 7, pp. 2332–2343, Jul. 2010.

[18] O. Dordevic, M. Jones, and E. Levi, "A space-vector PWM algorithm for a three-level seven-phase voltage source inverter," in *Proc. Eur. Power Elec. Conf.*, Birmingham, U.K., 2011 [CD-ROM], Paper 0123, pp. 1–11.

[19] O. López, J. Alvarez, J. Doval-Gandoy, and F. D. Freijedo, "Multilevel multiphase space vector PWM algorithm," *IEEE Trans. Ind. Electron.*, vol. 55, no. 5, pp. 1933–1942, May 2008.

[20] O. López, J. Alvarez, J. Doval-Gandoy, and F. D. Freijedo, "Multilevel multiphase space vector PWM algorithm with switching state redundancy," *IEEE Trans. Ind. Electron.*, vol. 56, no. 3, pp. 792–804, Mar. 2009.

[21] J. I. Leon, S. Vaquez, J. A. Sanchez, R. Portillo, L. G. Franquelo, J. M. Carrasco, and E. Dominguez, "Conventional space-vector modulation techniques versus the single-phase modulator for multilevel converters," *IEEE Trans. Ind. Electron.*, vol. 57, no. 7, pp. 2473–2482, Jul. 2010.

[22] D. Dujic, M. Jones, and E. Levi, "Generalized space vector PWM for sinusoidal output voltage generation with multi-phase voltage source inverters," *Int. J. Ind. Elec. Drives*, vol. 1, no. 1, pp. 1–13, 2009.

[23] D. Dujic, M. Jones, and E. Levi, "Continuous carrier-based versus space vector PWM for five-phase VSI," in *Proc. IEEE: Int. Conf. Comput. Tool EUROCON*, Warsaw, Poland, 2007, pp. 1772–1779.

[24] O. Dordević, N. Bodo, and M. Jones, "Model of an induction machine with an arbitrary phase number in MATLAB\SIMULINK for educational use," in *Proc. Int. Universities Power Eng. Conf.*, Cardiff, U.K., 2010 [CD-ROM], Paper 222, pp. 1–6.

[25] M. Jones, S. Vukosavic, D. Dujic, and E. Levi, "A synchronous current control scheme for multiphase induction motor drives," *IEEE Trans. Energy Convers.*, vol. 24, no. 4, pp. 860–868, Dec. 2009.

**Emil Levi** (S'89–M'92–SM'99–F'09) received the M.Sc. and Ph.D. degrees from the University of Belgrade, Belgrade, Yugoslavia, in 1986 and 1990, respectively.

From 1982 to 1992, he was with the Department of Electrical Engineering, University of Novi Sad. In May 1992, he joined Liverpool John Moores University, Liverpool, U.K.,where in September 2000 he became a Professor of Electric Machines and Drives.

Dr. Levi serves as an Editor of the IEEE TRANSACTION ON ENERGY CONVERSION, a Co-Editor-in-Chief of the IEEE TRANSACTION ON INDUSTRIAL ELECTRONICS, and as the Editor-in-Chief of the IET Electric Power Applications. He is the recipient of the Cyril Veinott Award of the IEEE Power and Energy Society for 2009 and the Best Paper Award of the IEEE TRANSACTION ON INDUSTRIAL ELECTRONICS for 2008.

**I Nyoman Wahyu Satiawan** was born in Singaraja, Bali, Indonesia, in 1970. He received the Graduate's degree in electrical engineering from the University of Udayana, Bali and the M.Sc. degree in control engineering from the Liverpool John Moores University, Liverpool, U.K., in 1996 and 2001, respectively. He joined University of Mataram, West Nusa Tenggara, Indonesia, as an academic in 1998. He is currently working toward the Ph.D. degree at Liverpool John Moores University, Liverpool, U.K.

His research interests include the area of electric motor drives and power converters.

**Nandor Bodo** (S'11) received the Master's degree in power, electronic and telecommunication engineering in 2009 in Power Electronics Area from the Faculty of Technical Sciences, University of Novi Sad, Novi Sad, Serbia. He is currently working toward the Ph.D. degree at the Liverpool John Moores University, Liverpool, U.K.

His research interests include power electronics and variable speed drives.

**Martin Jones** received the B.Eng. degree (First Class Hons.) from the Liverpool John Moores University, Liverpool, U.K., in 2001. He was a Research Student at the Liverpool John Moores University from September 2001, when he received the Ph.D. degree. He was a recipient of the IEE Robinson Research Scholarship during his Ph.D. studies.

He is currently with Liverpool John Moores University as a Reader. His research interest includes area of high performance ac drives.

# 11. IEEETEC2012_A Space-Vector Modulation Scheme for Multilevel

ORIGINALITY REPORT

| 20% | 13% | 19% | 8% |
|---|---|---|---|
| SIMILARITY INDEX | INTERNET SOURCES | PUBLICATIONS | STUDENT PAPERS |

PRIMARY SOURCES

| | | |
|---|---|---|
| 1 | Martin Jones, Milan Darijevic, Emil Levi. "Decoupled modulation techniques for a four-level five-phase open-end winding drive", 2014 IEEE Energy Conversion Congress and Exposition (ECCE), 2014<br>Publication | 15% |
| 2 | mafiadoc.com<br>Internet Source | 5% |

| | | | |
|---|---|---|---|
| Exclude quotes | On | Exclude matches | < 5% |
| Exclude bibliography | On | | |

# 11. IEEETEC2012_A Space-Vector Modulation Scheme for Multilevel

GRADEMARK REPORT

FINAL GRADE

/0

GENERAL COMMENTS

**Instructor**

PAGE 1

PAGE 2

PAGE 3

PAGE 4

PAGE 5

PAGE 6

PAGE 7

PAGE 8

PAGE 9

PAGE 10